Time-resolved photoluminescence study of excitons in hexagonal GaN layers grown on sapphire

S. Pau, Z. X. Liu, and J. Kuhl
Max-Planck-Institut für Festkörperforschung, Heisenbergstrasse 1, 70569 Stuttgart, Germany

J. Ringling and H. T. Grahn
Paul-Drude-Institut für Festkörperelektronik, Hausvogteiplatz 5-7, D-10117 Berlin, Germany

M. A. Khan and C. J. Sun
APA Optics Inc., 2950 N. E. 84th Lane, Blaine, Minnesota 55449

O. Ambacher and M. Stutzmann
Walter-Schottky-Institut, Technische Universität München, D85748 Garching, Germany
(Received 15 May 1997; revised manuscript received 9 September 1997)

We performed time-resolved and continuous wave photoluminescence on two samples of hexagonal GaN, one with free exciton emission and the other without. For the sample with free exciton emission, very different decay dynamics are observed between the front and backside emission. We find that the strain caused by the lattice mismatch between the sapphire substrate and the GaN film has a large influence on the population decay of the sample with free exciton emission and a minor influence on the decay properties of the sample dominated by bound exciton emission. A polariton picture is used to describe the observed behavior.
[S0163-1829(98)09109-7]

I. INTRODUCTION

Recent advances in GaN as a wide band-gap light emitter have generated much interest in the study of the basic properties of GaN.[1] It is hoped that a precise knowledge of the intrinsic GaN parameters will lead to improvements in device design and fabrication. Time-resolved photoluminescence (TRPL) is a powerful experimental tool to study new materials primarily because of the large amounts of spectral and temporal information one can obtain from such experiment. Several groups have performed TRPL on the wurzite and cubic phase of GaN using either single photon counting or a streak camera.[2–5] Most studies have been done on samples where the recombination was dominated by bound excitons at low temperature.[5] The purpose of this paper is to present a systematic study of both free and bound excitons of hexagonal GaN for different temperature, excitation intensity, and sample quality. We show that the emission characteristics are highly dependent on the crystal quality of the sample and explain the widespread values of the excitonic recombination lifetime that have been published in the literature by using the polariton picture.

II. EXPERIMENTAL SETUPS AND SAMPLES

The measurements are done using a Hamamatsu Syncroscan streak camera with a temporal and a spectral resolution of 10 ps and 0.36 nm, respectively. For TRPL excitation, we utilize the third harmonic of the mode-locked Ti:Sapphire laser at 260 nm with an approximate pulse width of 150 fs and a spot diameter of 50 μm. For CW excitation, we use the 325 nm line of the HeCd laser. We perform TRPL on two nominally undoped samples grown on $c-Al_2O_3$ substrates. Sample A has a thickness of 3.8 μm, a room-temperature electron concentration of 5×10^{16} cm^{-3}, and an electron mobility of 600 cm^2/Vs. At low temperature, the dominant emission is from the donor-bound exciton (DX) and the A and B free excitons. The full width at half maximum of the DX line is 1.7 meV at 10 K, and the sample is taken from the same wafer as the sample in Ref. 6. The epitaxial GaN films are deposited using low-pressure metalorganic chemical vapor deposition on the basal plane of the sapphire substrates. The deposition is carried out at 100 mbars and 1050 °C using triethylgallium and ammonia. A thin (50–100 nm) AlN buffer layer was grown at 700 −800 °C prior to the GaN film.[7] In contrast, sample B with a thickness of 3.3 μm, a room-temperature electron concentration of 2×10^{17} cm^{-3}, and an electron mobility of 280 cm^2/Vs has no observable free exciton emission. The GaN film on sample B was grown by plasma-induced molecular-beam epitaxy (PIMBE) using a conventional effusion cell for gallium and a rf-plasma atomic radical source (Oxford Applied Research CARS-25) for nitrogen. The inductively coupled plasma power was 400 W and the pressure in the MBE chamber during growth was 4×10^{-5} mbars. The sample was grown at 800 °C with a growth rate of 0.5 μm/h.[8] The strong DX emission from sample B at 5 K has a linewidth of 5 meV. CW photoluminescence and reflectivity measurements at 10 K show negligible Stokes shift in sample A and a 5 meV Stokes shift in sample B, indicating large inhomogeneous broadening and trap density. Both samples are polished on the backside to improve optical transmission.

III. RESULTS

In bulk material, the $k=0$ exciton forms an exciton polariton which is a stationary state of the system. As was first pointed out by Hopfield,[9] it is improper to talk about radia-

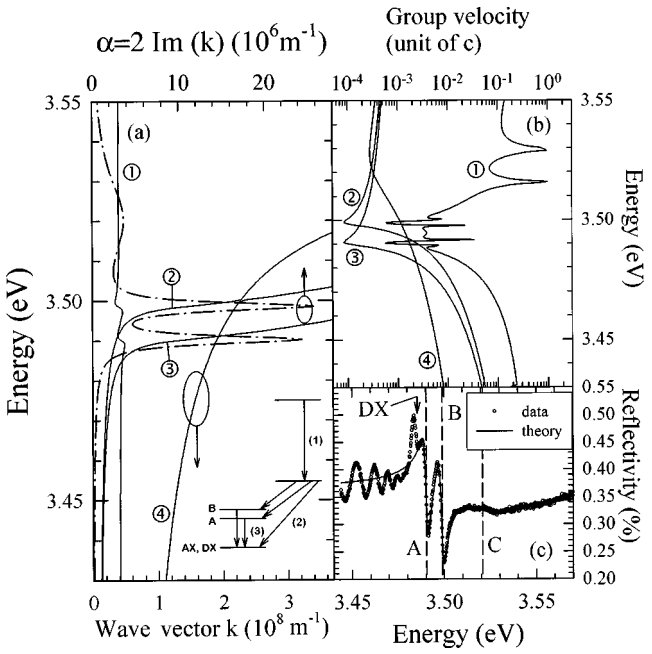

FIG. 1. (a) Theoretical polariton dispersion (solid curves) and theoretical absorption $\alpha=2\ \mathrm{Im}(k)$ (dashed-dotted curve). The inset shows the three-step model that describes the system. (b) Polariton group velocity for different branches. (c) Reflectivity spectra of sample A.

tive lifetime for the free exciton in bulk material. The relevant idea is that the exciton forms stationary polariton states, and the leakage of the polariton from the interfaces of the bulk leads to observable emission outside the sample.[10,11] Thus, a measurement of the emission is a direct probe of the polariton population. The rate of the emission is determined by the polariton leakage rate and the polariton population decay rate.

The polariton dispersion is given by

$$\varepsilon(k,\omega)=\varepsilon_\infty+\sum_i \frac{4\pi\alpha_i\omega_{0i}^2}{\omega_{0i}^2+(\hbar^2\omega_{0i}/m_i)k^2-\omega^2-i\Gamma_i\omega}, \quad (1)$$

where $\varepsilon_\infty=5.35$ is the high-frequency dielectric constant. ω_{0i}, $4\pi\alpha_i$, Γ_i, and m_j are the resonance frequency, polarizability, effective linewidth, and effective mass of the ith exciton. Figure 1(a) shows the theoretical four-branches polariton dispersion and absorption calculated using Eq. (1) and the parameters: $4\pi\alpha=2.272\times10^{-3}$, 2.345×10^{-3}, 3.314×10^{-3}, $\hbar\omega_0=3.4899$, 3.4983, and 3.5202 eV, and $\Gamma=2.478$, 2.532, and 26.52 meV for the A, B, and C excitons, respectively. The energies, linewidths, and polarizabilities are that of sample A and is calculated using a least-square fit of the reflectivity spectrum using Eq. (1) and the Pekar boundary conditions[12]. In the fit, we assume that all the effective masses are equal to the electron mass, $m_i=m_0$, that the excitons dead layer thickness is 12 nm, and that the GaN slab is sufficiently thick near the resonance energies so that the system can be treated as two semi-infinite regions. Although such a many parameters fit (nine parameters in our case) gives accurate values of ω_0, it can only give an order of magnitude estimate of the intrinsic polarizabilities of the free exciton as evidenced by the varying values reported in the literature.[13,14] The main reasons for this are the different quality of samples that are used by different groups and the sensitivity of the reflectivity fit to the actual potential of the surface boundary seen by the excitons.[15] The theoretical absorption agreed well with the experimental absorption.[16] In Fig. 1(b), we plot the group velocity of the different polariton branches given by $v_g=\hbar^{-1}\partial E(k)/\partial k$. In the vicinity of the exciton resonances, the propagation velocity can be drastically reduced with a maximal value of $c/2n$ where n is the GaN background refractive index. For a 2–3 μm sample such as ours, we expect that the time for the polariton to propagate across the sample is of the order of 0.1 to 1 ps which is much shorter than any decay rate observed in our experiment. Thus, we can neglect any transient polariton propagation effect in the intepretation of the exciton-polariton dynamics in our system.

The experimental reflectivity spectrum and the theoretical-fitting of sample A are plotted in Fig. 1(c). We identify the dominant transitions to be the A and B free excitons. The DX exciton contributes a small ''wiggle'' in the reflectance spectrum due to its finite absorption and there

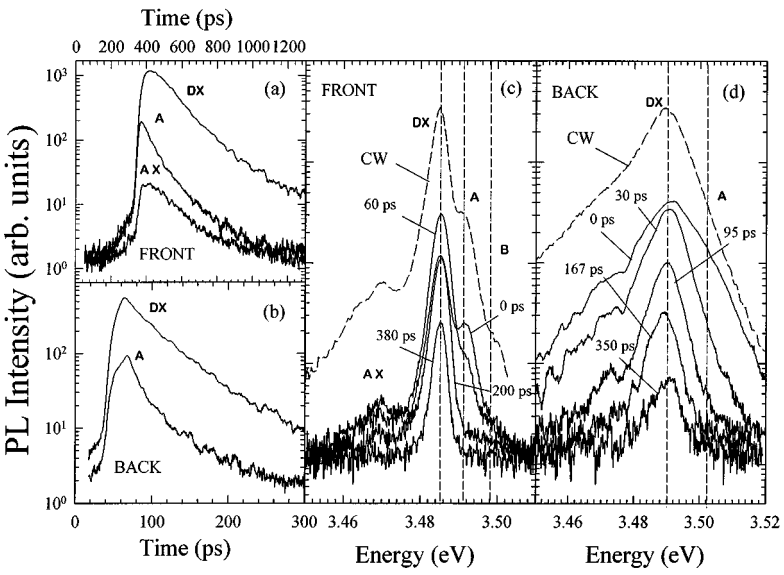

FIG. 2. TRPL of sample A, (a) Decay of the DX, AX, and A excitons at excitation power of 90 μW as measured from the front side. (b) Decay of DX and A excitons as measured from the back side. PL Spectrum at different times after initial excitation as measured from the front (c) and back (d) sides. Dashed lines show the PL spectra under CW excitation. Note that the relative scale between the CW and time-resolved PL intensities are arbitrary.

exists no Stokes shift between the free exciton resonances and the photoluminescence (PL) peaks in Fig. 2. We consider the decay dynamics of sample A when the sample is excited from the front and the backsides. Figure 2(a) shows the low-temperature decay dynamics of the different excitons for sample A. A fit to a single exponential of the form, $A+Be^{-t/\tau}$, shows that the decay times τ are 162, 136, and 66 ps for the AX, DX, and A excitons, respectively. We have found that the PL spectrum several 10 ps after initial excitation [Fig. 2(c)] is very similar to the PL spectrum obtained under CW excitation. This suggests that the different exciton branches are in thermal equilibrium with each other on a time scale less than 10 ps of initial excitation. To understand the different decay rates of the excitons, we consider the following process in the polariton picture [see the inset of Fig. 1(a)]. Initially, (1) hot carriers and excitons are created by the short pulse. These carriers thermalize to the polariton bottleneck region [the shoulders of the dispersion labeled 2, 3, and 4 in Fig. 1(a)] after about 10–20 ps by emission of LO and acoustic phonons. In Ref. 17, this thermalization process was shown to be dominated by an indirect process with simultaneous emission of LO phonons. Subsequently (2) the thermalized excitons are transfered to the $k\simeq 0$ polariton states. The leakage of these polaritons or scattering from impurity and interfaces result in a thermalized PL emission after the initial few tens of picoseconds. Simultaneously, (3) part of the thermalized exciton population and $k\simeq 0$ polariton states are trapped by impurities. The impurity-bound exciton subsequently decays either radiatively or nonradiatively. For low impurity density, the decay rate of the AX and DX lines are limited by the capture rate to the bound exciton state.

Different dynamical responses are observed depending on whether the emission is measured from the front (GaN) side or the back (Al_2O_3) side of the sample. Figure 2(b) shows decay dynamics when the sample is excited and measured from the backside. A fit to a single exponential shows that the decay times are 88 and 16 ps for the DX and A excitons, respectively. These rates are independent of the excitation intensity range in our experimental setup ($\sim 1-100$ μW). Figure 2(c) shows the corresponding emission spectrum at different times. Despite the observation that the PL is uniform across the sample position from the same side, very different behavior is observed on the back emission. The difference is not attributed to a signal distortion from the thick Al_2O_3 substrate layer since we have measured the transmission of a bare Al_2O_3 sample and find it to be over 85% uniform over the energy range of interest. All measurements in Fig. 2 are taken at 4.5 K under identical excitation conditions. In comparison with the front emission, the back emission has a larger linewidth and has a peak emission that is shifted 5 meV to the blue side. For bulk material in which polariton scattering by defects is large, the photoluminescence signal comes predominately from the top layer of a thickness of $1/\alpha$ at the interface of the material, where α is the absorption coefficient. For GaN and excitation far above the bandgap, this is less than 100 nm. In this respect, the different emission dynamics between the front and backsides can be interpreted as a consequence of the sample inhomogeneity at the two interfaces. This is particularly true for GaN that is grown on Al_2O_3 where considerable lattice mismatch and strain on the back surface exists. It has been shown that the strain in the GaN film is relaxed only for film with thickness above 150 μm.[18] Compressive strain on the backside leads to a localized increase of the GaN bandgap. The broadened line shapes and the blue shifts are consequences of these residual strain fields caused by differences in the thermal-expansion coefficients of the layers and has been observed for samples of different thicknesses in the front emission.[13,19,20] We believe the predominant emission from the backside are from the GaN layer and not from the AlN buffer layer which has a bandgap of 6.28 eV at 5 K.[1]

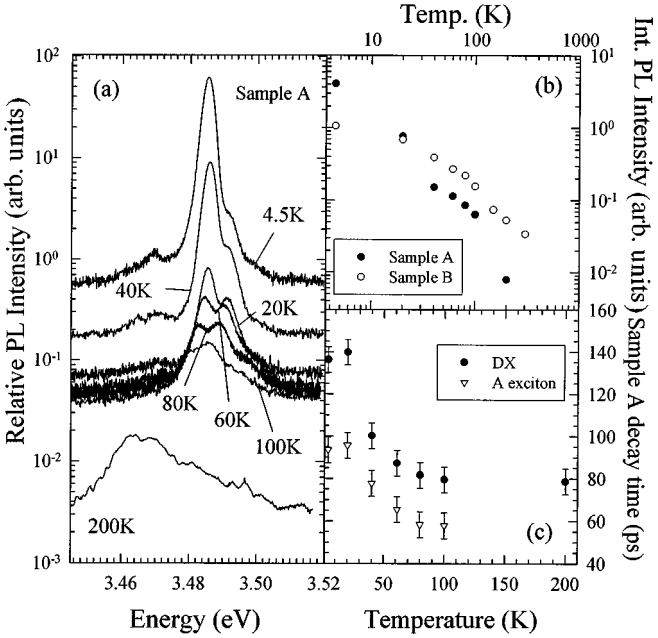

FIG. 3. (a) Temporally integrated spectra taken at different temperatures for sample A. (b) Temporally and spectrally integrated PL intensity at different temperatures for sample A and B. (c) Decay time of DX and A excitons at different temperatures for sample A.

In the polariton picture, the decay rate is expected to be the same for observation from the front and back surfaces. This is analogous to the photon lifetime of a two-mirrors laser cavity. For such a cavity, the photon lifetime depends only on the mirror reflectivities and is the same whether it is measured outside one of the mirrors or the other. For the polariton in a slab, the decay of the polariton should also be identical even though the polariton trapping rate and the polariton leakage rate can be very different at the two sides. Our observation of the different polariton decay rates at the front and back sides implies that the polariton, once formed at the front interface by the above-mentioned process, does not propagate to the other interface. Otherwise, the decay rates of the front and backsides should be identical. We expect that the polariton from one interface is highly damped in the vicinity of the other interface because of the large difference in exciton energies (of the order of 5 meV) or polariton detuning caused by residual strain near the two interfaces. For the front side where the polariton energy is smaller, propagation to the backside requires transition to higher energy where the polariton density of state is high. This process requires absorption of phonon and is unlikely at low temperature. For the substrate side where the polariton energy is higher, as deduced from the blue shift between the front and

back emission, propagation to the front side is feasible by emission of acoustic phonons. This propagation constitutes an additional decay mechanism for the polariton and can lead to a faster decay rate as we observed from the TRPL of the backside.

Figure 3(a) shows the time-integrated PL of the front emission of sample A at different temperatures. We observe the characteristic redshift of the emission with increasing temperature which is caused by the decrease of the GaN bandgap and broadening of the PL linewidth. The latter is caused by an increase of phonon scattering. The integrated spectral and temporal emission of the free excitons are reduced by three orders of magnitude from 4.5 K to room temperature [Fig. 3(b)]. The decrease in emission efficiency is primarily caused by trapping of carriers by impurities and defects and the subsequent nonradiative recombination at a longer wavelength. Although the density of traps is constant, the trapping rate increases with temperature because of the increased phonon scattering rate. Thus, most of the hot carriers and hot excitons generated by the laser pulse are trapped before any formation of a $k=0$ exciton. At temperatures where $k_BT \gtrsim E_b$ ($T>230$ K), where E_b is the exciton binding energy, the $k=0$ excitons are no longer stable due to thermal dissociation. Figure 3(c) shows the DX and A exciton decay time of sample A at various temperatures from the front side. The rapid decrease of the DX lifetime with increasing temperature confirms our assignment that it is a shallow-donor-bound exciton and is consistent with the observation by another group.[3] The $k=0$ polariton lifetime at the A exciton energy also decreases with temperature. In general, there are two contributions to the polariton decay rate, the polariton leakage rate and the polariton trapping rate. For a fixed temperature, the polariton leakage rate is highly sample specific because the rate depends mainly on the interface properties. The polariton trapping rate increases with temperature because of increasing phonon scattering which leads to increased trapping of polaritons by impurities and other nonradiative recombination processes. Our interpretation of the decay dynamics explains qualitatively the different free exciton decay rates observed by different research groups, since the quality of the GaN which plays a crucial role in determining the leakage rate can be very different depending on growth conditions. As we have shown, the rate can even be very different for the same sample depending on whether the PL is excited from the free surface or the substrate side.

Figure 4(a) shows the TRPL for sample B at 5 K. In comparison with sample A, the relative emission from the DX exciton is much stronger. A weak shoulder at 3.485 eV suggests the presence of a small population of A excitons. The PL spectrum at very short times after initial excitation is very similar to the CW PL (dashed line), implying that full thermalization occurs within the risetime of 10 ps. The decay near the DX state can be very well fitted by a single exponential. A plot of the decay time across the inhomogeneous distribution is shown in Fig. 4(b). At the low-energy side, the decay time is constant and of the order of 55 ps. For fast impurity capture rate such as in this sample, this time can be interpreted as the bound exciton radiative lifetime. A similar lifetime has been observed for the DX state by another group.[3] At the high-energy side near the free exciton energy,

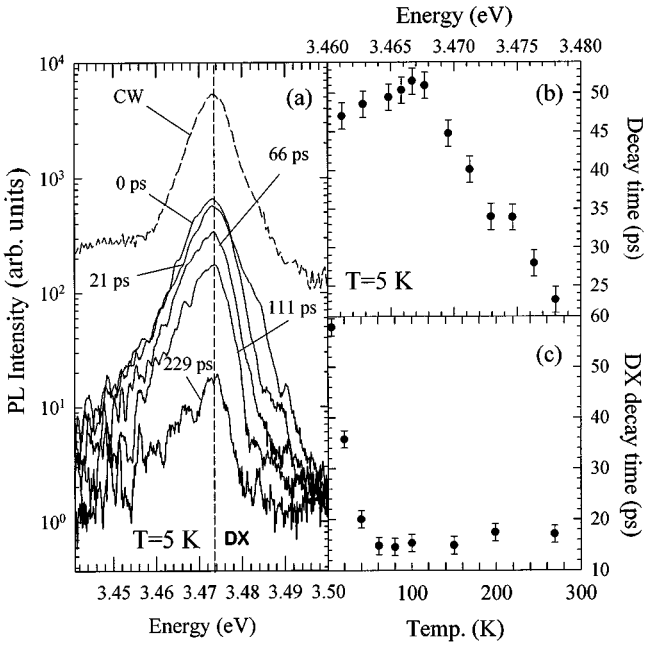

FIG. 4. TRPL of sample B, (a) PL spectra at different times after initial excitation. The dashed line shows the PL under CW excitation. (b) Exponential decay time at different energies of the inhomogeneous line. (c) Donor-bound exciton (DX) decay time at different temperatures.

the decay rate is of the order of 20 ps. Both leakage rate of the exciton polariton and impurity trapping rate contribute to this decay rate which gives an upper bound of the impurity capture rate. In our experiment, we find no change in the decay rate for our range of excitation powers. The decay of the DX line is found to increase rapidly with temperature due to ionization by acoustic-phonon scattering [Fig. 4(c)] and is similar to the observation in sample A. In terms of the polariton picture, the initial hot carriers transform into thermal excitons within 10 ps. The high density of defects and impurities acts as an efficient trap for the thermal excitons before any appreciable formation of exciton polaritons. At low temperature, the broad distribution of impurity states decay radiatively within 55 ps. A similar decay is observed on the backside suggesting that the strain induced at the GaN sapphire interface plays a less important role in this case.

IV. CONCLUSION

The decay dynamics of bulk GaN near the excitonic resonances must be described in terms of the polariton picture. In a high-quality sample, the relevant parameters are the polariton formation time (rise time of the decay) and the leakage rate of the polariton (lifetime of the decay). We have shown that the decay rate depends strongly on crystal quality within a layer of thickness $1/\alpha$ as seen from the different observed for between the front and backside emissions. In samples with a large trap density, the relevant parameters are the trapping time of thermal excitons by defects (decay rate at the high-energy side) and the radiative lifetime of the impurity bound excitons. The interface plays a less important role in this case.

ACKNOWLEDGMENT

S. P. thanks T. Ruf and K. Syassen for helpful discussions.

[1] B. Monemar, Semicond. Semimet. **50**, 305 (1997); H. Morkoç *et al.*, J. Appl. Phys. **76**, 1363 (1994).
[2] M. Smith *et al.*, Appl. Phys. Lett. **67**, 3387 (1995); J. P. Bergman *et al.*, in *Gallium Nitride and Related Materials*, edited by R. D. Dupuis *et al.*, MRS Symposia Proceedings No. 395 (Materials Research Society, Pittsburgh, 1996), p. 709.
[3] A. Hangleiter *et al.*, in *Gallium Nitride and Related Materials*, (Ref. 2), p. 559.
[4] R. Klann *et al.*, Phys. Rev. B **52**, R11 615 (1995); Appl. Phys. Lett. **70**, 1808 (1997).
[5] L. Eckey *et al.*, Appl. Phys. Lett. **68**, 415 (1996); Y. Kawakami *et al.*, *ibid.* **69**, 1414 (1996); G. D. Chen *et al.*, J. Appl. Phys. **79**, 2675 (1996); W. Shan *et al.*, Appl. Phys. Lett. **69**, 740 (1996).
[6] M. Smith *et al.*, J. Appl. Phys. **79**, 7001 (1996).
[7] M. A. Khan, J. N. Kuzina, J. M. Van Hove, and D. T. Olson, Appl. Phys. Lett. **58**, 526 (1991).
[8] H. Angerer, O. Ambacher, R. Dimitrov, T. Metzger, W. Rieger, and M. Stutzmann, MRS Internet J. Nitride Semicond. Res. **1**, 15 (1996).
[9] J. J. Hopfield, Phys. Rev. **112**, 1555 (1958).
[10] P. Wiesner and U. Heim, Phys. Rev. B **11**, 3071 (1975).
[11] H. Sumi, J. Phys. Soc. Jpn. **41**, 526 (1976).
[12] Y. Chen, B. Gil, and H. Mathieu, Ann. Phys. (Paris) **12**, 109 (1987).
[13] M. Tchounkeu *et al.*, J. Appl. Phys. **80**, 5352 (1996).
[14] W. Shan *et al.*, Phys. Rev. B **54**, 16 369 (1996).
[15] J. Lagois, Phys. Rev. B **23**, 5577 (1987).
[16] J. Baranowski *et al.*, in *III-V Nitrides*, edited by F. A. Ponce, T. D. Moustakis, I. Akasaki, and B. A. Monemar, MRS Symposia Proceedings No. 449 (Materials Research Society, Pittsburgh, 1997), p. 393.
[17] D. Kovalev *et al.*, Phys. Rev. B **54**, 2518 (1996).
[18] T. Detchprohm, K. Hiramtsu, K. Itoh, and I. Akasaki, Jpn. J. Appl. Phys., Part 2 **31**, L1454 (1992).
[19] W. Shan *et al.*, Phys. Rev. B **54**, 13 460 (1996).
[20] D. Volm *et al.*, Phys. Rev. B **53**, 16 543 (1996).